Computational Analysis of the Solvent Effect on the Barrier to Rotation about the Conjugated C−N Bond in Methyl *N*,*N*-Dimethylcarbamate

Paul R. Rablen

Department of Chemistry, Swarthmore College, 500 College Avenue, Swarthmore, Pennsylvania 19081-1397

prablen1@swarthmore.edu

Received June 22, 2000

It is known experimentally that, in contrast to the case of amides, barriers to rotation about the conjugated C−N bonds of carbamates show very little solvent dependence. Calculations of the relative solvation energies of the equilibrium and transition state structures of methyl *N*,*N*-dimethylcarbamate (MDMC) and *N*,*N*-dimethylacetamide (DMA) were carried out using a continuum reaction field model in order to investigate the reason that bulk solvent polarity raises the barrier for DMA but leaves the barrier for MDMC unchanged. The results confirmed that MDMC is insensitive to bulk solvent polarity, probably as a result of the relatively small molecular dipole moment. Calculations of proton affinities and of the strength of association with a single water molecule were then performed in order to investigate why hydrogen-bond-donating solvents affect DMA but not MDMC. These calculations showed that MDMC is a less capable hydrogen-bond acceptor than DMA, and that the rotational barrier of MDMC does not increase in response to protonation or hydrogen-bonding nearly as much as the barrier of DMA does. Both of these factors contribute to making the rotational barrier of MDMC insensitive to solvent hydrogen-bond donor ability.

Introduction

Rotation about the conjugated C−N bond in amides has long held interest for chemists.[1−6] The barrier to rotation, which is unusually high for a single bond, reveals a great deal about electronic structure. Furthermore, the behavior of amide bonds has important consequences in biological chemistry. For instance, peptide bond isomerization in proline residues can limit the rate of protein folding,[7] and one of the apparent roles of rotamase enzymes is to catalyze this isomerization.[7,8]

Solvent effects have also received considerable attention.[9] While most reactions are carried out in solution, many common ideas about reactivity implicitly pertain to isolated molecules and thus the gas phase. Furthermore, molecular orbital calculations, which are ever more widely used, yield predictions that are strictly valid only for the gas phase. Application of such calculations to reactions and structures in solution requires an understanding of the solvent's influence. These motivations drive the large body of ongoing research on solvent effects and quantitative solvation models.

Amide bond rotation is generally retarded by polar solvents, as has been shown in numerous experimental and computational studies. Particularly detailed data are available for the case of *N*,*N*-dimethylacetamide (DMA) (**1a**).[2,5,10−14] DMA has two possible transition states, since the nitrogen becomes pyramidalized, and consequently the lone pair can point in a direction either syn or anti to the carbonyl oxygen.

The transition state structure of DMA having the lone pair anti to the carbonyl (DMA TS1, **2a**) is favored in the gas phase and in aprotic solvents, although calculations suggest that the "syn" structure (**3a**) might be competitive or even preferred in aqueous solution.[11]

Ab initio calculations consistently indicate that the equilibrium structure has a somewhat larger dipole moment than the disfavored transition state structure (TS2) and a much larger dipole moment than the favored

(1) Orville-Thomas, W. J. *Internal Rotation in Molecules*; John Wiley & Sons: New York, 1974.

(2) (a) Stewart, W. E.; Siddall, T. H., III. *Chem. Rev.* **1970**, *70*, 517−551 and references therein. (b) Drakenberg, T.; Dahlqvist, K. J.; Forsen, S. *J. Phys. Chem.* **1972**, *76*, 2178−2183.

(3) (a) Cox, C.; Lectka, T. *J. Org. Chem.* **1998**, *63*, 2426−2427. (b) Cox, C.; Young, V. G., Jr.; Lectka, T. *J. Am. Chem. Soc.* **1997**, *119*, 2307−2308. (c) Cox, C.; Ferraris, D.; Murthy, N. N.; Lectka, T. *J. Am. Chem. Soc.* **1996**, *118*, 5332−5333.

(4) Kessler, H. *Angew. Chem., Int. Ed. Engl.* **1970**, *9*, 219−235.

(5) For example, Neugebauer Crawford, S. M.; Taha, A. N.; True, N. S.; LeMaster, C. B. *J. Phys. Chem. A* **1997**, *101*, 4699−4706.

(6) Wiberg, K. B.; Breneman, C. M. *J. Am. Chem. Soc.* **1992**, *114*, 831−840.

(7) (a) Schmid, F. X. In *Protein Folding*; Creighton, T. E., Ed.; W. H. Freeman: New York, 1992; pp 197−241; see also other chapters in this book. (b) Schmid, F. X.; Mayr, L. M.; Mücke, M.; Schönbrunner, E. R. *Adv. Protein Chem.* **1993**, *44*, 25−66. (c) Eberhardt, E. S.; Loh, S. N.; Hinck, A. P.; Raines, R. T. *J. Am. Chem. Soc.* **1992**, *114*, 5437−5439 and references therein. (d) Stein, R. L. *Adv. Protein Chem.* **1993**, *44*, 1−24.

(8) (a) Schreiber, S. L. *Science* **1991**, *251*, 283−287. (b) Gething, M.-J.; Sambrook, J. *Nature* **1992**, *355*, 33−45. (c) Fischer, G.; Schmid, F. X. *Biochemistry* **1990**, *29*, 2205−2212.

(9) Reichardt, C. *Solvents and Solvent Effects in Organic Chemistry*, 2nd ed.; VCH Publishers: Germany, 1988.

(10) Suarez, C.; LeMaster, C. B.; LeMaster, C. L.; Tafazzoli, M.; True, N. S. *J. Phys. Chem.* **1990**, *94*, 6679−6683.

(11) Duffy, E. M.; Severance, D. L.; Jorgensen, W. L. *J. Am. Chem. Soc.* **1992**, *114*, 7535−7542.

(12) Gao, J. *J. Am. Chem. Soc.* **1993**, *115*, 2930−2935. Gao, J. *Proc. Indian Acad. Sci.* **1994**, *106*, 507.

(13) Perrin, C. L.; Thoburn, J. D.; Kresge, A. J. *J. Am. Chem. Soc.* **1992**, *114*, 8800−8807.

(14) Wiberg, K. B.; Rablen, P. R.; Rush, D. J.; Keith, T. A. *J. Am. Chem. Soc.* **1995**, *117*, 4261−4270.

10.1021/jo000945z CCC: $19.00
Published on Web 10/25/2000

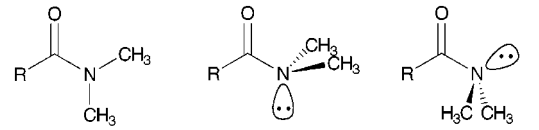

equilibrium structure, ES | anti transition state structure, TS1 | syn transtion state structure, TS2

R = CH_3: **1a** R = OCH_3: **1b** | R = CH_3: **2a** R = OCH_3: **2b** | R = CH_3: **3a** R = OCH_3: **3b**

transition state structure (TS1).[14] Simple electrostatic considerations then predict that a polar environment should raise the barrier, and indeed experimental measurements have confirmed this prediction.[2,14] Moreover, the magnitude of the solvent effect agrees closely with the predictions of a polarizable continuum reaction field model, at least for certain "well-behaved" aprotic solvents that lack second-row elements and aromatic rings.[14] According to this model, the magnitude of the solvent effect has a very nearly linear dependence on the Onsager dielectric function, defined as $(\epsilon - 1)/(2\epsilon + 1)$, where ϵ is the dielectric constant.[15] Others have attributed the observed solvent effects to solvent internal pressure and to the greater volume requirements of the transition state structures in comparison to the equilibrium structure.[10]

Protic solvents such as methanol and water further increase the observed barriers to rotation substantially beyond what would be predicted on the basis of the dielectric constants alone. This effect has been attributed to hydrogen-bond donation by the solvent. The hydrogen-bonding interaction between a single water molecule and the carbonyl oxygen of DMA is presumably stronger for the more polarized equilibrium structure than for the transition state structure, thus leading to an increase in the barrier height.[11,14]

Carbamates are close structural relatives of amides. Like amides, carbamates have conjugated C−N bonds with fairly high barriers to rotation.[3] The barriers are somewhat smaller than in amides, however, because the strength of the interaction between the nitrogen lone pair and the carbonyl group is reduced by the competing interaction between the opposing oxygen atom and the same carbonyl. One of the oxygen lone pairs is able to donate into the carbonyl π system and thereby partially compensate for the loss of π interaction with the nitrogen lone pair when C−N bond rotation takes place.

Carbamates might have been expected to show the same retardation of bond rotation in polar and hydrogen-bond donor solvents as is observed for amides. However, a recent study by Lectka and co-workers has shown this not to be the case.[3] Instead, the free energy barriers $\Delta G^{\ddagger}$ in a number of carbamates were observed to be almost invariant with the solvent, showing an increase of at most 0.3 kcal/mol on going from the least to the most polar environments. Table 1 summarizes some of the most relevant experimental data. The computational study presented here seeks to explain this striking difference in behavior between amides and carbamates.

Table 1. Experimental Rotational Barriers ($\Delta G^{\ddagger}$, kcal/mol) of Carbamates and Amides in Various Solvents

solvent	ϵ^a	carbamate[b]	amide[c]
gas phase	1.00		15.33[d]
cyclohexane	2.02		16.38
carbon tetrachloride	2.23	15.5	16.89
benzene	2.27		17.26
toluene	2.38		17.25
butyl ether	3.06		16.65
dichloromethane	9.08		17.95
acetone	20.70		17.49
acetonitrile	36.70	15.3	17.77
methanol	32.66	15.5	18.71
methanol−water mixtures		15.5−15.6	
water	78.38		19.05

[a] Dielectric constant at 25 °C (298 K); Source: *CRC Handbook of Chemistry and Physics*, 74th ed. (1993−1994); Lide, D. R., Ed. in Chief; CRC Press, Inc.: Boca Raton, FL, 1993. [b] Activation free energies for *N*,*N*-dimethylacetamide (DMA) at 298 K, taken from ref 14. [c] Activation free energies for methyl *N*-benzyl-*N*-methylcarbamate at 298 K, taken from ref 3a. [d] Gas-phase barrier for DMA obtained from the kinetic data reported in Ross, B. D.; True, N. S.; Matson, G. B. *J. Phys. Chem.* **1984**, *88*, 2675; analysis of data as per ref 14.

Calculations

The Gaussian 94[16] and Gaussian 98[17] packages were used to carry out all ab initio MO calculations. Standard Pople basis sets[18] were utilized, although in some cases with customized augmentation. The nonstandard augmentations were originally adapted from the work of Ochterski,[19] and the use of these basis sets for the calculation of hydrogen-bonded complexes has been described elsewhere.[20] The (d+) and (2d+) descriptors indicate an additional set of diffuse d polarization functions having an exponent 1/4 as large as that for the previous set. The basis sets 6-31+G(d(X+),p) and 6-31++G(2d(X+),p) include the additional diffuse polarization functions only on atoms having lone pairs (e.g., *not* on C or H).

Density functional calculations employed the B3LYP keyword, which invokes Becke's 3-parameter hybrid method[21] using the correlation functional of Lee, Yang, and Parr.[22,23] In some cases, energy differences are reported that are the average of B3LYP[21−23] and MP2[24] calculations with large basis sets. This procedure has been recommended by Turecek, who has found that such averages yield excellent agreement with the highest

(15) (a) Onsager, L. *J. Am. Chem. Soc.* **1936**, *58*, 1486-1493. (b) Kirkwood, J. G. *J. Chem. Phys.* **1934**, *2*, 351−361. (c) Born, M. *Z. Phys.* **1920**, *1*, 45−48.

(16) Frisch, M. J.; Trucks, G. W.; Schlegel, H. B.; Gill, P. M. W.; Johnson, B. G.; Robb, M. A.; Cheeseman, J. R.; Keith, T.; Petersson, G. A.; Montgomery, J. A.; Raghavachari, K.; Al-Laham, M. A.; Zakrzewski, V. G.; Ortiz, J. V.; Foresman, J. B.; Cioslowski, J.; Stefanov, B. B.; Nanayakkara, A.; Challacombe, M.; Peng, C. Y.; Ayala, P. Y.; Chen, W.; Wong, M. W.; Andres, J. L.; Replogle, E. S.; Gomperts, R.; Gonzalez, C.; Martin, R. L.; Fox, D. J.; Binkley, J. S.; Defrees, D. J.; Baker, J.; Stewart, J. P.; Head-Gordon, M.; Gonzalez, C.; Pople, J. A. *Gaussian 94* (Revision C.2); Gaussian, Inc.: Pittsburgh, PA, 1995.

(17) Frisch, M. J.; Trucks, G. W.; Schlegel, H. B.; Scuseria, G. E.; Robb, M. A.; Cheeseman, J. R.; Zakrzewski, V. G.; Montgomery, J. A. Jr.; Stratmann, R. E.; Burant, J. C.; Dapprich, S.; Millam, J. M.; Daniels, A. D.; Kudin, K. N.; Strain, M. C.; Farkas, O.; Tomasi, J.; Barone, V.; Cossi, M.; Cammi, R.; Mennucci, B.; Pomelli, C.; Adamo, C.; Clifford, S.; Ochterski, J.; Petersson, G. A.; Ayala, P. Y.; Cui, Q.; Morokuma, K.; Malick, D. K.; Rabuck, A. D.; Raghavachari, K.; Foresman, J. B.; Cioslowski, J.; Ortiz, J. V.; Stefanov, B. B.; Liu, G.; Liashenko, A.; Piskorz, P.; Komaromi, I.; Gomperts, R.; Martin, R. L.; Fox, D. J.; Keith, T.; Al-Laham, M. A.; Peng, C. Y.; Nanayakkara, A.; Gonzalez, C.; Challacombe, M.; Gill, P. M. W.; Johnson, B.; Chen, W.; Wong, M. W.; Andres, J. L.; Gonzalez, C.; Head-Gordon, M.; Replogle, E. S.; Pople, J. A. *Gaussian 98* (Revision A.6); Gaussian, Inc.: Pittsburgh, PA, 1998.

(18) Hehre, W. J.; Radom, L.; Schleyer, P. v. R.; Pople, J. A. *Ab Initio Molecular Orbital Theory*; Wiley: New York, 1986.

(19) Ochterski, J. W. Ph.D. Thesis, Wesleyan University, 1994.

(20) Rablen, P. R.; Lockman, J. W.; Jorgensen, W. L. *J. Phys. Chem. A* **1998**, *102*, 3782−3797.

(21) Becke, A. D. *J. Chem. Phys.* **1993**, *98*, 5648−5652.

(22) Lee, C.; Yang, W.; Parr, R. G. *Phys. Rev. B* **1988**, *37*, 785−789.

(23) Miehlich, B.; Savin, A.; Stoll, H.; Preuss, H. *Chem. Phys. Lett.* **1989**, *157*, 200−206.

levels of ab initio theory for the calculation of proton affinities.[25]

Geometry optimizations were carried out without constraints. All stationary points were confirmed as minima or saddle points (transition states), as appropriate, via vibrational frequency calculations. Zero-point vibrational energies were scaled by 0.8934 at the Hartree−Fock level[26] and by 0.97 at the B3LYP level.[20]

The effect of bulk solvent was simulated using the IPCM continuum reaction field model,[27] with the isodensity contour set to 0.0004 electrons per cubic bohr.[28] The influence of hydrogen-bonding in water and, by extension, other protic solvents was explored by calculating the strength of association of the solute, in either its equilibrium geometry or the transition state geometry, with a single water molecule. The influence of protic solvents was also studied by calculating the proton affinities of the equilibrium structure and of the transition state structures of the solute. Both of these approaches have been used previously for similar purposes, using some of the same levels of calculation as are given here.[14,29]

Results

To explore the effects of nonspecific, bulk solvation on the rotational barriers of carbamates, calculations were carried out on methyl *N*,*N*-dimethylcarbamate (MDMC) (**1b**), representing a typical carbamate, using a continuum reaction field model to represent the solvent. Reaction field theory, first developed by Onsager and Kirkwood, provides a simple model for calculating the bulk electrostatic component of solvation energies.[15] The solvent is treated as a continuum characterized only by a static dielectric constant, ϵ, and a cavity in which the solute is situated. The electrical moments of the solute cause the continuum to become polarized, and the resulting electrostatic interactions between the solute and the medium lead to stabilization. The model neglects terms in the solvation energy associated with formation of the cavity. However, for conformational isomerization reactions the cavity is unlikely to change much over the course of the reaction, and so this shortcoming is of little consequence for the current application.

Reaction field theory has been adapted for use with ab initio MO calculations in the form of self-consistent reaction field (SCRF) theory, so-called because the reaction field component of the energy is incorporated directly into the Hamiltonian, and the molecular wave function is thus optimized in a manner that includes the solvation energy.[30−33] The most recent versions of the Gaussian ab initio MO package incorporate several versions of reaction field theory, including the isodensity polarizable continuum model (IPCM) and self-consistent IPCM (SCIPCM) implementations.[31,34] In both cases, the molecular wave function is used to define the solvent−solute interface, i.e., the surface at which the dielectric constant abruptly drops to zero. Previous work has shown that the 0.0004 electron per cubic Bohr electron density surface serves as an appropriate definition of the boundary, and yields satisfactory agreement with experiment for a variety of systems.[14,27,35] The choice of 0.0004 as the isodensity contour enjoys the additional advantage that the enclosed volumes correlate closely with experimental molecular volumes.[35]

Table 2. Calculated IPCM Solvent Effects for Methyl *N*,*N*-Dimethylcarbamate (kcal/mol)[a]

dielectric constant	rotational Barrier			solvent effect[e]
	TS1[b]	TS2[c]	effective[d]	
1.0	12.86	13.67	12.75	0.00
2.0	12.88	13.82	12.80	+0.05
3.0	12.86	13.88	12.78	+0.03
5.0	12.81	13.92	12.74	−0.01
10.0	12.74	13.95	12.68	−0.07
78.0	12.65	13.98	12.61	−0.14

[a] Calculated at MP2/6-311++G**(6D)//MP2/6-31+G*, with HF/6-31G* ZPE scaled by 0.8934. [b] TS1 has the nitrogen lone pair anti to the carbonyl oxygen. [c] TS2 has the nitrogen lone pair syn to the carbonyl oxygen. [d] Effective total transition state energy, taking into account both TS1 and TS2 at 273 K. [e] Difference in effective total transition state energy at a given dielectric constant and at $\epsilon = 0$.

The results obtained from applying the IPCM procedure are listed in Table 2. Continuum models have in fact proven effective for estimating solvent effects under many, although not all, circumstances.[14,35−38] The isodensity polarizable continuum models implemented in the Gaussian 98 package in particular have been shown to reproduce solvent effects on the barriers to rotation of conjugated C−N bonds in amides and related compounds quite accurately for aprotic solvents that lack second-row elements and aromatic rings.[14,29] According to these models, the magnitude of the solvent effect has a very nearly linear dependence on the Onsager dielectric function, defined as $(\epsilon - 1)/(2\epsilon + 1)$, where ϵ is the dielectric constant.[15] The MP2/6-311++G**(6D)//MP2/6-31+G* level of theory used for the calculations on MDMC is the same as that used previously for DMA[14] and for a vinylogous nitrile.[29]

(24) (a) Møller, C.; Plesset, M. S. *Phys. Rev.* **1934**, *46*, 618−622. (b) Head-Gordon, M.; Pople, J. A.; Frisch, M. J. *Chem. Phys. Lett.* **1988**, *153*, 503−506. (c) Frisch, M. J.; Head-Gordon, M.; Pople, J. A. *Chem. Phys. Lett.* **1990**, *166*, 275−280. (d) Frisch, M. J.; Head-Gordon, M.; Pople, J. A. *Chem. Phys. Lett.* **1990**, *166*, 281−289. (e) Head-Gordon, M.; Head-Gordon, T. *Chem. Phys. Lett.* **1994**, *220*, 122−128. (f) Saebo, S.; Almlöf, *J. Chem. Phys. Lett.* **1989**, *154*, 83−89.

(25) Turecek, F. *J. Phys. Chem. A* **1998**, *102*, 4703−4713.

(26) Curtiss, L. A.; Raghavachari, K.; Trucks, G. W.; Pople, J. A. *J. Chem. Phys.* **1991**, *94*, 7221−7230.

(27) Foresman, J. B.; Keith, T. A.; Wiberg, K. B.; Snoonian, J.; Frisch, M. J. *J. Phys. Chem.* **1996**, *100*, 16098−16104.

(28) Wiberg, K. B.; Keith, T. A.; Frisch, M. J.; Murcko, M. *J. Phys. Chem.* **1995**, *99*, 9072−9079.

(29) Rablen, P. R.; Pearlman, S. A.; Miller, D. A. *J. Am. Chem. Soc.* **1999**, *121*, 227−237.

(30) (a) Rinaldi, D.; Rivail, J. L. *Theor. Chim. Acta* **1973**, *32*, 57. (b) Tapia, O.; Goscinski, O. *Mol. Phys.* **1975**, *29*, 1653−1661. (c) Rivail, J. L.; Terryn, B.; Ruiz-López, M. F. *J. Mol. Struct. (THEOCHEM)* **1985**, *120*, 387.

(31) Cf. Wong, M. W.; Frisch, M. J.; Wiberg, K. B. *J. Am. Chem. Soc.* **1991**, *113*, 4776−4782. Wong, M. W.; Wiberg, K. B.; Frisch, M. J. *J. Chem. Phys.* **1991**, *95*, 8991−8998.

(32) Rinaldi, D.; Ruiz-Lopez, M. F.; Rivail, J.-L. *J. Chem. Phys.* **1983**, *78*, 834−838.

(33) (a) Miertus, S.; Scrocco, E.; Tomasi, J. *Chem. Phys*, **1981**, *55*, 117−129. (b) Alagona, G.; Ghio, C.; Igual, J.; Tomasi, J. *J. Am. Chem. Soc.* **1989**, *111*, 3417−3421. (c) Tomasi, J.; Bonaccorsi, R.; Cammi, R.; Valle, F. O. J. *J. Mol. Struct.* **1991**, *234*, 401−424. (d) Alagona, G.; Ghio, C.; Igual, J.; Tomasi, J. *J. Mol. Struct. (THEOCHEM)* **1990**, *63*, 253−283. (e) Mennucci, B.; Tomasi, J. *J. Chem. Phys.* **1997**, *106*, 5151−5158, and references therein.

(34) Barone, V.; Cossi, M. *J. Phys. Chem. A* **1998**, *102*, 1995−2001.

(35) Wiberg, K. B.; Keith, T. A.; Frisch, M. J.; Murcko, M. *J. Phys. Chem.* **1995**, *99*, 9072−9079.

(36) (a) Giesen, D. J.; Gu, M. Z.; Cramer, C. J.; Truhlar, D. G. *J. Org. Chem.* **1996**, *61*, 8720−8721. (b) Chambers, C. C.; Hawkins, G. D.; Cramer, C. J.; Truhlar, D. G. *J. Phys. Chem.* **1996**, *100*, 16385−16398.

(37) Still, W. C.; Tempczyk, A.; Hawley, R. C.; Hendrickson, T. *J. Am. Chem. Soc.* **1990**, *112*, 6127−6129.

(38) For reviews of continuum solvation models, see: (a) Tomasi, J.; Persico, M. *Chem. Rev.* **1994**, *94*, 2027−2094. (b) Cramer, C. J.; Truhlar, D. G. *Rev. Comput. Chem.* **1990**, *6*, 1−72.

Table 3. Dipole Moments (Debye)

compound	structure[a]	μ[b]
DMA	ES	4.04
	TS1	2.08
	TS2	3.63
MDMC	ES	2.55
	TS1	0.91
	TS2	2.80

[a] TS1 has the nitrogen lone pair anti to the carbonyl oxygen, and TS2 has the nitrogen lone pair syn to the carbonyl oxygen; ES is the equilibrium structure. [b] B3LYP/6-31++G(2d(X+),p)//B3LYP6-31+G(d(X+),p) dipole moment in Debye.

Table 4. Calculated Proton Affinities (kcal/mol)

structure[a]	position of protonation[b]	proton affinity			
		HF[c]	DFT[d]	MP2[e]	B3/MP2[f]
DMA	O/anti	−217.0	−216.1	−213.4	−214.7
	O/syn	−214.3	−213.5	−210.6	−212.1
	N	−205.0	−202.4	−202.4	−202.4
DMA TS1	O/anti	−194.7	−194.6	−188.6	−191.6
	O/syn	−194.1	−194.3	−188.0	−191.1
	N	−218.1	−218.6	−217.0	−217.8
DMA TS2	O/anti	−196.0	−195.9	−190.2	−193.0
	O/syn	−201.9	−200.9	−195.7	−198.3
	N	−221.0	−220.5	−219.0	−219.8
MDMC	O/anti	−207.6	−208.1	−204.6	−206.3
	O/syn	−208.7	−208.6	−205.2	−206.9
	N	−204.8	−202.7	−202.7	−202.7
MDMC TS1	O/anti	−193.6	−194.2	−188.8	−191.5
	O/syn	−197.4	−197.3	−192.0	−194.7
	N	−219.5	−218.8	−217.5	−218.1
MDMC TS2	O/anti	−194.2	−194.8	−189.3	−192.0
	O/syn	−203.5	−202.2	−197.6	−199.9
	N	−219.7	−218.6	−217.4	−218.0

[a] TS1 has the nitrogen lone pair anti to the carbonyl oxygen, and TS2 has the nitrogen lone pair syn to the carbonyl oxygen. [b] "Anti" and "syn" are relative to the nitrogen atom. [c] HF/6-31+G*, including ZPE scaled by 0.8934. [d] B3LYP/6-311+G(2df,p)//B3LYP/6-31+G**, including B3LYP/6-31+G** ZPE scaled by 0.97. [e] MP2/6-311+G(2df,p)//B3LYP/6-31+G**, including B3LYP/6-31+G** ZPE scaled by 0.97. [f] Average of DFT and MP2 values (previous two columns).

As a further aid to understanding the influence of bulk solvent polarity, the calculated gas-phase dipole moments of DMA and MDMC are reported in Table 3. Roughly speaking, solvation energy in a polarizable continuum model is expected to be proportional to the square of the dipole moment of the solute, so long as the size of the solute remains constant.[15]

To understand the effect of solvent hydrogen-bond donor ability on the rotational barrier of MDMC, two additional sets of calculations were performed. First, as shown in Tables 4 and 5, the proton affinities of the equilibrium structures and transition state structures of both DMA and MDMC were computed. Protonation may be regarded as the limiting extreme of hydrogen-bonding, and so it was hoped that these calculations would shed light upon the effects of hydrogen-bonding on the rotational barriers in these systems. Several levels of calculation were used, including HF/6-31+G*, B3LYP/6-311+G(2df,p)//B3LYP/6-31+G**, and MP2/6-311+G(2df,p)//B3LYP/6-31+G**. The average of the latter two calculations, which is also reported in Tables 4 and 5, has been shown by Turecek to yield remarkably good agreement with the highest levels of calculation for the prediction of proton affinities.[25] Examination of Tables 4 and 5 reveals that all the methods of calculation yield the same trends.

Table 5. Calculated Rotational Barriers of Protonated Species (kcal/mol)

cmpd	transition state[a]	position of protonation[b]	rotational barrier			
			HF[c]	DFT[d]	MP2[e]	B3/MP2[f]
DMA	TS1	none	13.0	16.2	14.6	15.4
		O/anti	35.4	37.7	39.4	38.5
		O/syn	33.3	35.5	37.2	36.3
		N	0.0	0.0	0.0	0.0
	TS2	none	17.1	19.2	17.8	18.5
		O/anti	38.1	39.4	41.1	40.2
		O/syn	29.5	31.8	32.7	32.3
		N	1.2	1.1	1.2	1.1
MDMC	TS1	none	14.7	15.2	14.1	14.6
		O/anti	28.6	29.1	29.9	29.5
		O/syn	25.9	26.5	27.2	26.9
		N	0.0	−0.9	−0.8	−0.8
	TS2	none	15.4	16.0	14.8	15.4
		O/anti	28.8	29.3	30.1	29.7
		O/syn	20.6	22.4	22.4	22.4
		N	0.5	0.0	0.0	0.0

[a] TS1 has the nitrogen lone pair anti to the carbonyl oxygen, and TS2 has the nitrogen lone pair syn to the carbonyl oxygen. [b] "Anti" and "syn" are relative to the nitrogen atom. [c] HF/6-31+G*, including ZPE scaled by 0.8934. [d] B3LYP/6-311+G(2df,p)//B3LYP/6-31+G**, including B3LYP/6-31+G** ZPE scaled by 0.97. [e] MP2/6-311+G(2df,p)//B3LYP/6-31+G**, including B3LYP/6-31+G** ZPE scaled by 0.97. [f] Average of DFT and MP2 values (previous two columns).

Table 6. Calculated Energies of Interaction with a Single Water Molecule (kcal/mol)

structure[a]	position of interaction[b]	interaction energy	
		DFT/B1[c]	DFT/B2[d]
DMA	O/anti	−5.30	−5.05
	O/syn	−4.65	−4.39
	N	−1.02	−0.86
DMA TS1	O/anti	−3.88	−3.71
	O/syn	−3.60	−3.42
	N	−4.14	−3.84
DMA TS2	O/anti	−4.13	−3.95
	O/syn	−3.93	−3.79
	N	−4.90	−4.68
MDMC	O/anti	−4.47	−4.30
	O/syn	−4.27	−4.09
	N	−0.84	−0.70
MDMC TS1	O/anti	−3.76	−3.61
	O/syn	−3.72	−3.55
	N	−4.30	−4.05
MDMC TS2	O/anti	−3.78	−3.58
	O/syn	−3.64	−3.50
	N	−4.57	−4.30

[a] TS1 has the nitrogen lone pair anti to the carbonyl oxygen, and TS2 has the nitrogen lone pair syn to the carbonyl oxygen. [b] "Anti" and "syn" are relative to the nitrogen atom. [c] B3LYP/6-31+G(d(X+),p), including ZPE scaled by 0.97. [d] B3LYP/6-31++G(2d(X+),p)//B3LYP/6-31+G(d(X+),p), including B3LYP/6-31+G(d(X+),p) ZPE scaled by 0.97.

Finally, calculations were performed of the complexes formed from a single water molecule hydrogen-bonding with DMA or MDMC, at the B3LYP/6-31++G(2d(X+),p)//B3LYP/6-31+G(d(X+),p) level of theory. This density functional procedure has been demonstrated previously to yield excellent relative energies for hydrogen-bonded complexes of polar organic molecules with water.[20] The interaction energies are presented in Tables 6 and 7, and the optimized geometries are shown in Figures 1 and 2. These calculations provide a somewhat more realistic estimate of the effect of hydrogen-bonding in water solution. Again, calculations were performed for both the equilibrium structures and the transition state structures of DMA and MDMC.

Table 7. Calculated Rotational Barriers of Hydrogen-Bonded Species (kcal/mol)

cmpd	transition state[a]	position of interaction[b]	rotational barrier DFT/B1[c]	rotational barrier DFT/B2[d]
DMA	TS1	none	16.12	15.94
		O/anti	17.53	17.28
		O/syn	17.17	16.90
		N	13.00	12.95
	TS2	none	19.07	18.87
		O/anti	20.23	19.97
		O/syn	19.79	19.47
		N	15.19	15.04
MDMC	TS1	none	15.02	14.73
		O/anti	15.72	15.42
		O/syn	15.57	15.27
		N	11.56	11.39
	TS2	none	15.85	15.55
		O/anti	16.53	16.27
		O/syn	16.47	16.14
		N	12.12	11.95

[a] TS1 has the nitrogen lone pair anti to the carbonyl oxygen, and TS2 has the nitrogen lone pair syn to the carbonyl oxygen. [b] "Anti" and "syn" are relative to the nitrogen atom. [c] B3LYP/6-31+G(d(X+),p), including ZPE scaled by 0.97. [d] B3LYP/6-31++G(2d(X+),p)//B3LYP/6-31+G(d(X+),p), including B3LYP/6-31+G(d(X+),p) ZPE scaled by 0.97.

Discussion

Effect of Solvent Polarity. B3LYP/6-31++G(2d-(X+),p)//B3LYP6-31+G(d(X+),p) calculations indicate that the preferred transition state structure of MDMC has a dipole moment of 0.91 D, compared to 2.55 D for the equilibrium structure (Table 3). This behavior qualitatively resembles that of amides such as DMA, for which the dipole moment of the favored transition state is 2.08 D and that of the equilibrium structure is 4.04 D. The substantially higher dipole moment of the equilibrium structure of DMA relative to the transition state structure leads to the expectation that bulk solvent polarity should significantly raise the barrier to rotation. In fact, experiment and theory agree that the barrier is about 2.3 kcal/mol higher in acetone or acetonitrile than it is in the gas-phase, or about 1.2 kcal/mol higher than it is in cyclohexane.[14] From this perspective, the lack of a solvent effect on the rate of bond rotation in carbamates such as MDMC seems somewhat surprising.

However, it must be borne in mind that, to a first approximation, bulk solvent stabilization increases as the square of the dipole moment.[15] In a reaction field model, the stabilization energy is understood as the interaction between the dipole moment of the molecule and the reflection dipole moment induced by the solute in the surrounding medium. However, the reflection dipole is itself directly proportional to the dipole moment of the solute, and so the overall interaction energy has a quadratic dependence on the molecular dipole moment.

The difference in dipole moment between the transition state and equilibrium structure is similar for MDMC (1.6 D) to what it is for DMA (2.0 D). However, the absolute values of the dipole moments are considerably larger for DMA. Consequently, in a quadratic model, the solvent effect is expected to be larger for DMA. In fact, plugging the dipole moments quoted above into a simple quadratic equation predicts that the solvent effect on bond rotation should be somewhat less than half as great for MDMC as for DMA.

In fact, the effect of a polar medium on MDMC is even smaller than suggested by the dipole moments. The influence of bulk solvent polarity can be quantified by applying the reaction field calculations discussed earlier. Table 2 shows the results of using the IPCM procedure to estimate the solvent effect on bond rotation in MDMC. The predicted consequence of a polar environment is negligible, in accord with experiment.[3] Interestingly, what small (less than 0.2 kcal/mol) effect is calculated to exist does not operate in a monotonic fashion with respect to the dielectric constant. The barrier first increases slightly, and then decreases, as the dielectric constant increases from 1 to 78. This behavior is strikingly different from that of DMA, for which the IPCM model correctly predicts that the barrier increases monotonically by ~2 kcal/mol on going from the gas phase to polar aprotic solvents such as acetone.[14]

Effect of Solvent Hydrogen-Bond Donor Ability. Solvent hydrogen-bond donor ability substantially increases the rotational barrier in DMA, over and above the effect of bulk solvent polarity. For instance, the rotational barrier in methanol is 1.0 kcal/mol higher than it is in acetonitrile, even though the dielectric constants are very similar.[14,39] This phenomenon is the result of two factors: hydrogen-bond donors associate strongly with the carbonyl group of DMA, and the presence of such hydrogen-bonds increases the barrier to rotation.

This behavior is illustrated by the data in Tables 4−7. Table 5 demonstrates that protonation of the carbonyl oxygen of DMA increases the rotational barrier from 15.4 to 38.5 kcal/mol. Protonation may be regarded as one extreme of a continuum representing acceptance of increasingly strong hydrogen-bonds. It is also possible to examine the effect of complexation of DMA with a single water molecule, and this information is presented in Tables 6 and 7. Table 6 shows that a water molecule interacts quite strongly with DMA (−5.1 kcal/mol) and preferentially at the carbonyl oxygen. Table 7 demonstrates that this complexation increases the rotational barrier by 1.3 kcal/mol. Not surprisingly, the effect is much smaller than for complete protonation.

However, as discussed earlier, dynamic NMR spectroscopy has shown that rotational barriers in carbamates such as MDMC are not increased by protic solvents.[3] The data in Tables 4−7 suggest that the absence of this behavior, which is so pronounced for DMA, results from two factors. First, hydrogen-bonding to MDMC has a smaller influence on the barrier than does hydrogen-bonding to DMA. Second, hydrogen-bonding to MDMC is slightly weaker, and therefore less prevalent in solution, than is hydrogen-bonding to DMA.

Effect of Hydrogen-Bond Formation on the Barrier to Bond Rotation. That hydrogen-bonding to the carbonyl of MDMC has a considerably smaller effect on the rotational barrier than does hydrogen-bonding to DMA is illustrated by the proton affinity calculations presented in Tables 4 and 5. Table 4 indicates that the most favorable position for protonation of the equilibrium structure of DMA is on the carbonyl oxygen, in a position anti to the amide nitrogen. Protonation at this site increases the rotational barrier by 23.1 kcal/mol, from 15.4 kcal/mol to 38.5 kcal/mol.

The most favorable position for protonation of MDMC is likewise on the carbonyl oxygen, but in a position syn to the nitrogen. Protonation of MDMC at this site

(39) In fact, acetonitrile has the higher dielectric constant: $\epsilon = 35.9$ for acetonitrile but $\epsilon = 32.7$ for methanol (source: ref 9).

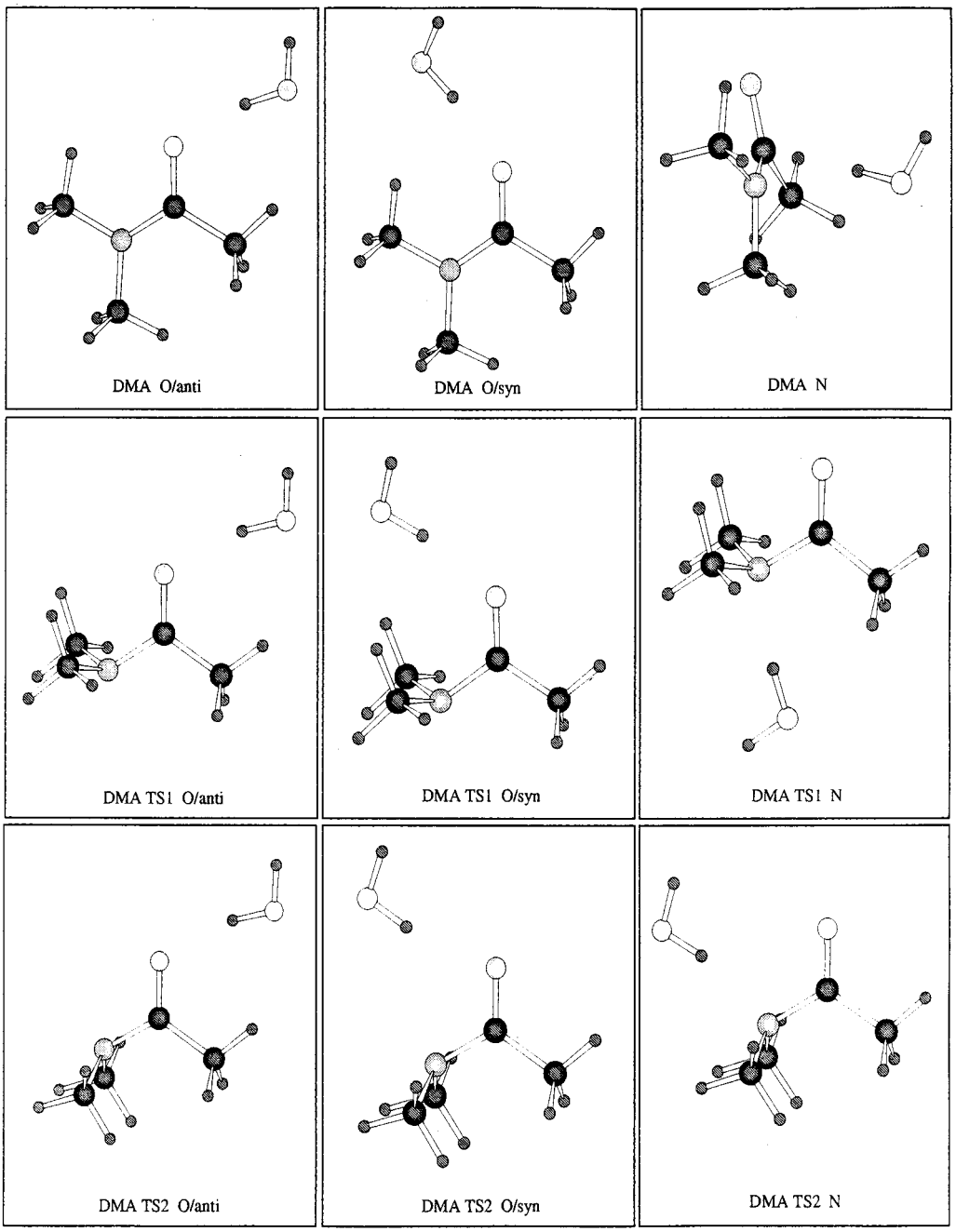

Figure 1. B3LYP/6-31+G(d(X+),p) optimized geometries of complexes of DMA with a single water molecule.

increases the C−N rotational barrier from 14.6 kcal/mol to 26.9 kcal/mol. This increase represents a difference of only 12.3 kcal/mol. Protonation of MDMC is thus only about half as effective at increasing the C−N rotational barrier as is protonation of DMA.

Protonation, of course, represents an extreme case, even if an informative one. A more realistic comparison to the environment in a protic solvent can be achieved by considering the interaction of a single water molecule with either DMA or MDMC. Table 6 lists the interaction energies for various possible geometries, while Table 7 provides the corresponding rotational barriers of the hydrogen-bonded complexes.

Table 6 demonstrates that DMA in its equilibrium geometry interacts most favorably with a water molecule if it is hydrogen-bonded to the carbonyl oxygen in a position anti to the nitrogen atom. This is the same position that is most favorable for protonation (Table 4). However, the interaction energy for hydrogen-bonding at this site decreases from 5.1 kcal/mol for the equilibrium structure to only 3.7 kcal/mol for the more favored transition state, so that hydrogen-bonding at this position increases the barrier from 15.9 kcal/mol to 17.3 kcal/mol.

The most favorable site for hydrogen-bonding in MDMC is also on the carbonyl oxygen in a position anti to the nitrogen atom (Table 6). This location differs slightly from the site of greatest basicity, which is on the carbonyl oxygen, but syn to the nitrogen atom (Table 4). The interaction energy at the favored anti position is 4.3 kcal/mol for the equilibrium structure and is 3.6 kcal/mol for the favored transition state. Thus hydrogen-bonding increases the barrier from 14.7 kcal/mol to 15.4 kcal/mol. This increase of 0.7 kcal/mol is only about half as great as the increase of 1.3 kcal/mol observed for DMA.

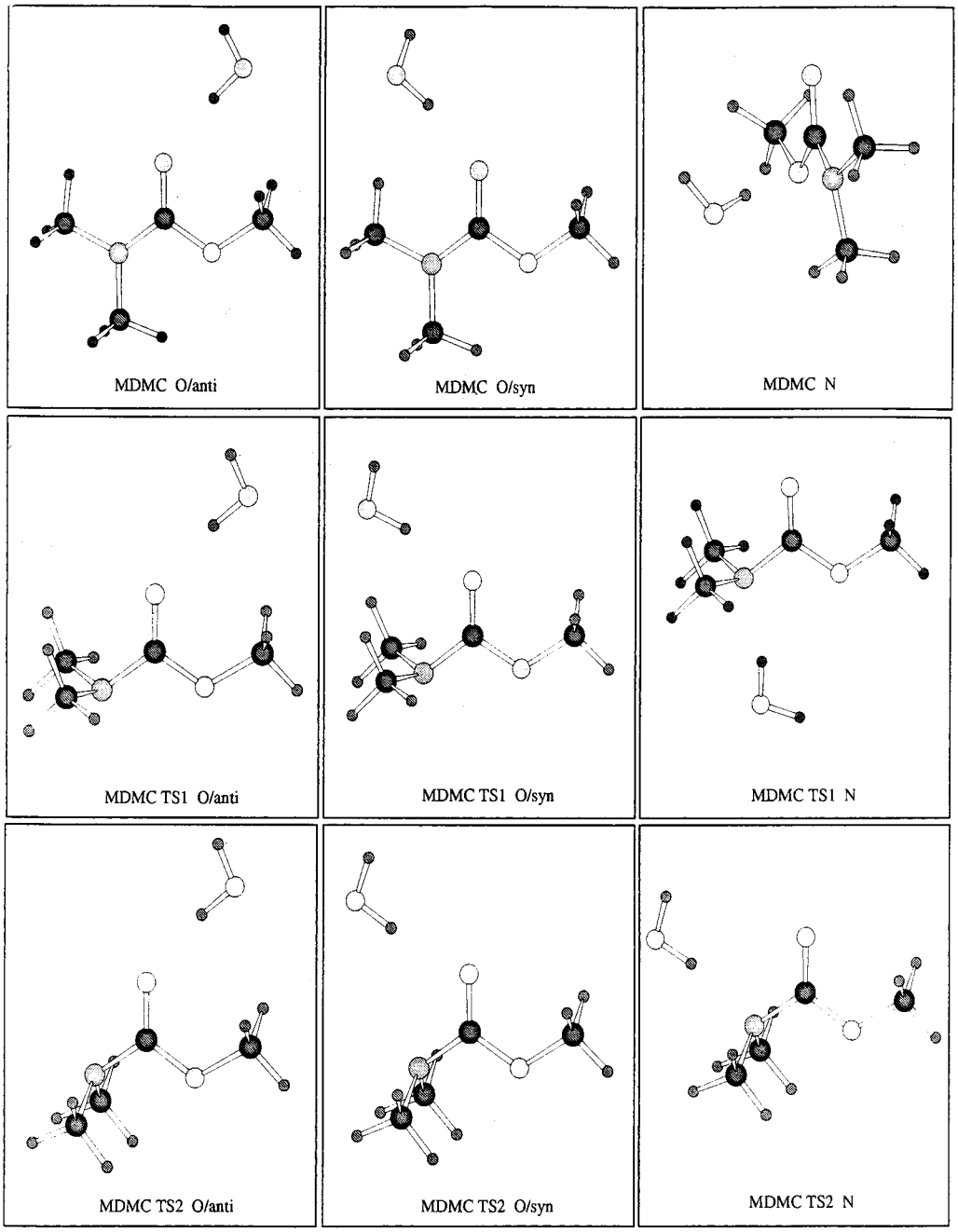

Figure 2. B3LYP/6-31+G(d(X+),p) optimized geometries of complexes of MDMC with a single water molecule.

Consistent with the proton affinity data discussed earlier, these calculations indicate that hydrogen-bonding is only about half as effective at increasing the rotational barrier in MDMC as in DMA.

Strength and Extent of Hydrogen-Bonding in Solution. The other reason for the striking difference in behavior between DMA and MDMC concerns the absolute strength of hydrogen-bonding, and therefore its prevalence in solution. MDMC is a weaker hydrogen-bond acceptor than is DMA. As a result, in protic solvents, MDMC is probably less extensively engaged in hydrogen-bonding than is DMA. This hypothesis is supported by two pieces of evidence that appear in Tables 4−7.

First, protonation of MDMC is considerably less favorable than is that of DMA, as shown in Table 4. The proton affinity of MDMC is 208.7 kcal/mol, but for DMA it is 217.0 kcal/mol. This difference is more significant than it might at first seem. To put these numbers in perspective, even a hydrocarbon such as ethylene has a proton affinity of 166.4 kcal/mol, while trimethylamine has a proton affinity of 228.3 kcal/mol.[40] Seen from this perspective, the difference between MDMC and DMA is substantial.

Second, the complexation energies of MDMC and DMA with a single water molecule, shown in Table 6, confirm that MDMC is a poorer hydrogen-bond acceptor than DMA. The most favorable interaction energy of MDMC with a water molecule is 4.3 kcal/mol, whereas for DMA the corresponding value is 5.1 kcal/mol. As the energy of interaction becomes less favorable, the extent of hydrogen-bonding to the carbonyl in protic solution decreases

(40) Calculated at the same (HF/6-31+G*) level of theory.

rapidly. Because of the competing influences of solvent−solvent hydrogen-bonding and entropy, the extent of solvent−solute hydrogen-bonding drops essentially to zero well *before* the gas-phase interaction energy becomes negligible.

When the interaction energy drops below a certain threshold, the solute is no longer a strong enough hydrogen-bond acceptor to compete effectively with solvent−solvent hydrogen-bonding. Thus the 0.8 kcal/mol difference in interaction energy between DMA and MDMC has a more dramatic effect on the extent of hydrogen-bonding in solution than might at first be suggested by the absolute ratio of the energies. The dimerization energy of water calculated at B3LYP/6-31++G(2d(X+),p)//B3LYP/6-31+G(d(X+),p) is 4.8 kcal/mol,[20] and perhaps this value can be taken as a very crude estimate of the "threshold energy" described above for water solution. It is worth noting that the hydrogen-bonding energy of DMA with water falls above this threshold, while the hydrogen-bonding energy of MDMC with water falls below it. This comparison provides further reason to believe that MDMC experiences substantially less hydrogen-bonding in solution than does DMA.

Summary

Unlike amides, carbamates such as MDMC show very little dependence of their C−N rotational barriers on the solvent. One reason polar solvents raise the barrier in DMA, a well-studied representative amide, is that the equilibrium structure has a substantially higher dipole moment than the preferred transition state. The dipole moment of MDMC, on the other hand, is much smaller than that of DMA. Since the solvation energy goes roughly as the square of the dipole moment, polar solvents affect the rotational barrier of MDMC much more weakly. This is so despite the fact that the transition state and the equilibrium structure have a dipole moment difference that is similar to the case of DMA. Reaction field calculations carried out using the IPCM model confirm that bulk polarizability of the medium does not significantly alter the rotational barrier, in excellent accord with the available experimental data.

The rotational barrier of DMA further increases when the solvent is a good hydrogen-bond donor, beyond what can be explained on the basis of bulk solvent polarity. This effect is easily understood as a consequence of hydrogen-bonding to the carbonyl oxygen, which is calculated to increase the rotational barrier. The rotational barriers of carbamates such as MDMC, on the other hand, are insensitive to whether the solvent is protic or aprotic. Two factors lead to this difference in behavior. First, MDMC is less prone to accepting hydrogen-bonds than is DMA. The lower affinity of MDMC for hydrogen-bonding, compared to DMA, is revealed by an 8 kcal/mol decrease in the calculated proton affinity. Furthermore, a single water molecule is calculated to associate 0.8 kcal/mol less strongly with MDMC than with DMA.

The second factor that makes carbamate bond rotation insensitive to solvent proton donor ability is that the rotational barrier does not change very much in response to a hydrogen-bond. Calculated proton affinities show that protonation of the carbonyl of MDMC increases the C−N rotational barrier by only 12.3 kcal/mol, compared with an increase of 23.1 kcal/mol in the case of DMA. Likewise, complexation with a single water molecule is calculated to increase the barrier by 1.3 kcal/mol for DMA, but only by 0.7 kcal/mol for MDMC.

Acknowledgment. Financial support for this work was provided by Swarthmore College and by a Faculty Start-up Grant for Undergraduate Institutions from the Camille and Henry Dreyfus Foundation. Acknowledgment is also made to the donors of the Petroleum Research Fund, administered by the American Chemical Society, for partial support of this research.

Supporting Information Available: Energies in Hartrees and optimized geometries for all the species represented in Tables 2−7, in *Z*-matrix form. This material is available free of charge via the Internet at http://pubs.acs.org.

JO000945Z